

Spectroscopic and Calorimetric Studies on the Mechanism of Methylene cyclopropane Rearrangements Triggered by Photoinduced Electron Transfer

Hiroshi Ikeda,^{*,†} Kimio Akiyama,[§] Yasutake Takahashi,^{†,||} Tatsuo Nakamura,[†] Satoshi Ishizaki,[†] Yukio Shiratori,[†] Hitoshi Ohaku,[†] Joshua L. Goodman,[‡] Abdelaziz Houmam,[⊥] Danial D. M. Wayner,[⊥] Shozo Tero-Kubota,[§] and Tsutomu Miyashi^{*,†}

Contribution from the Department of Chemistry, Graduate School of Science, Tohoku University, Sendai 980-8578, Japan, Institute of Multidisciplinary Research for Advanced Materials, Tohoku University, Sendai 980-8577, Japan, Department of Chemistry, University of Rochester, Rochester, New York 14627, and National Institute for Nanotechnology, National Research Council of Canada, Ottawa, Ontario, Canada K1A 0R6

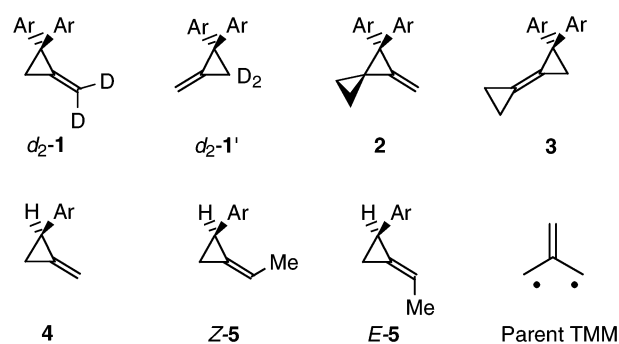
Received July 22, 2002; E-mail: ikeda@org.chem.tohoku.ac.jp

Abstract: 2-(Dideuteriomethylene)-1,1-bis(4-methoxyphenyl)cyclopropane (**d₂-1**) undergoes degenerate rearrangement in both singlet- and triplet-sensitized electron-transfer photoreactions. Nanosecond time-resolved absorption spectroscopy on laser flash photolysis of the unlabeled **1** with 9,10-dicyanoanthracene, 1,2,4,5-tetracyanobenzene, or *N*-methylquinolinium tetrafluoroborate as an electron-accepting photosensitizer gives rise to two transients with λ_{max} at 500 and 350 nm assigned to the dianisyl-substituted largely twisted trimethylenemethane cation radical (**6^{•+}**) and the corresponding diradical (**6^{••}**), respectively. These intermediates are also detected, respectively, by steady state and nanosecond time-resolved EPR with chloranil or anthraquinone as a sensitizer. The degenerate rearrangement of **d₂-1** thus proceeds via these two different types of intermediates in a cation radical cleavage–diradical cyclization mechanism. Energetics based on nanosecond time-resolved photoacoustic calorimetry support this mechanism. A comparison of the reactivities and the spectroscopic results of **1**, 1,1-bis(4-methoxyphenyl)-2-methylenespiro[2.2]pentane (**2**), and 1-cyclopropylidene-2,2-bis(4-methoxyphenyl)cyclopropane (**3**) suggest that the reversible methylenecyclopropane rearrangement between **2** and **3** proceeds via a similar mechanism.

Introduction

We have reported that 2,5-diaryl-3,3,4,4-tetradeuterio-1,5-hexadiene undergoes photoinduced electron-transfer (PET) degenerate Cope rearrangement, involving a 1,4-diarylcyclohexane-1,4-diyl cation radical and a 1,4-diarylcyclohexane-1,4-diyl.¹ An important reaction in this mechanism is the highly exergonic back electron transfer from a sensitizer anion radical to the 1,4-diarylcyclohexane-1,4-diyl cation radical to form the 1,4-diarylcyclohexane-1,4-diyl. In view of the expectation that the degenerate rearrangement of 2-(dideuteriomethylene)-1,1-bis(4-methoxyphenyl)cyclopropane (**d₂-1** in Chart 1)^{2,3} and the

Chart 1.^a



^a Abbreviation: Ar, 4-MeOC₆H₄; TMM, trimethylenemethane.

reversible methylenecyclopropane rearrangement between 1,1-bis(4-methoxyphenyl)-2-methylenespiro[2.2]pentane (**2**) and 1-cyclopropylidene-2,2-bis(4-methoxyphenyl)cyclopropane (**3**)³ occur by a similar mechanism, the PET reactions of 1,1-bis(4-methoxyphenyl)-2-methylenecyclopropane (**1**), **2**, and **3** were investigated by means of nanosecond time-resolved (TR) absorption spectroscopy, EPR, and photoacoustic calorimetry on laser flash photolysis. TR-EPR studies of **4** and (Z)- and (E)-1-ethylidene-2-(4-methoxyphenyl)cyclopropane (Z-**5** and

[†] Graduate School of Science, Tohoku University.

[§] Institute of Multidisciplinary Research for Advanced Materials, Tohoku University.

[‡] University of Rochester.

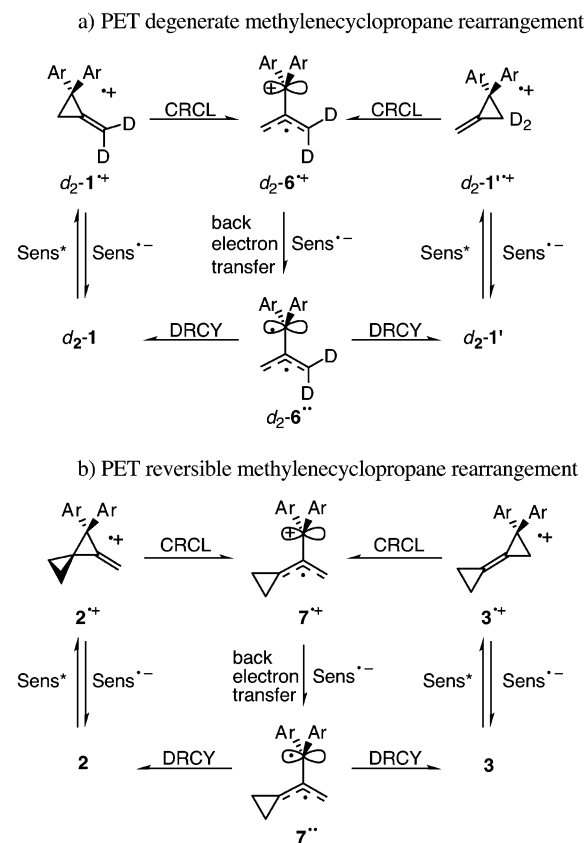
[⊥] National Research Council of Canada.

^{||} Present address: Department of Chemistry for Materials, Faculty of Engineering, Mie University.

(1) (a) Ikeda, H.; Minegishi, T.; Abe, H.; Konno, A.; Goodman, J. L.; Miyashi, T. *J. Am. Chem. Soc.* **1998**, *120*, 87–95. (b) Miyashi, T.; Ikeda, H.; Takahashi, Y. *Acc. Chem. Res.* **1999**, *32*, 815–824.

(2) Takahashi, Y.; Miyashi, T.; Mukai, T. *J. Am. Chem. Soc.* **1983**, *105*, 6511–6513.

(3) A part of this work was presented at the 8th IUPAC Conference on Physical Organic Chemistry (Japan, 1986)⁴ and at the 10th International Conference on Physical Organic Chemistry, Organic Chemistry Division, IUPAC (Israel, 1990)⁵ and reported as a preliminary communication.⁶

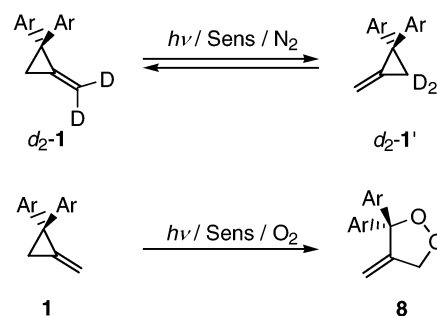
Scheme 1. CRCL–DRCY Mechanism for PET Methylenecyclopropane Rearrangement^a

^a Abbreviations: CRCL, cation radical cleavage; DRCY, diradical cyclization; PET, photoinduced electron transfer; Sens, sensitizer; Ar, 4-MeOC₆H₄.

E-5) established the stereochemical consequences for the initial ring cleavage to form a trimethylenemethane (TMM) cation radical intermediate. Herein we report spectroscopic and calorimetric evidence together with results of product analysis, which support the participation of two different types of intermediates in the PET methylenecyclopropane rearrangements of **1**, **2**, and **3** shown in Scheme 1.

Results and Discussion

PET Degenerate Rearrangement of *d*₂-1 and Reversible Methylenecyclopropane Rearrangement between **2 and **3**.** We have reported the degenerate rearrangement of *d*₂-**1** and oxygenation of **1** triggered by PET using a triplet sensitizer such as chloranil (CA) or anthraquinone (AQ).^{2,7} For spectroscopic convenience⁸ in laser flash photolyses, electron-transfer photoreactions of *d*₂-**1** and oxygenations of **1** were investigated using a singlet sensitizer such as 9,10-dicyanoanthracene (DCA), 1,2,4,5-tetracyanobenzene (TCNB), or *N*-methylquinolinium tetrafluoroborate (NMQ⁺BF₄[−]) (Scheme 2).

Scheme 2. Degenerate Methylenecyclopropane Rearrangement of *d*₂-**1** and Oxygenation of **1** Triggered by PET^a

^a Sens: DCA, TCNB, or NMQ⁺BF₄[−].

Table 1. Halfwave Oxidation Potentials (*E*^{ox}_{1/2}) of **1**, Free Energy Changes (ΔG_{et}) Associated with Electron-Transfer Reactions of **1** with the Excited State of Sensitizers, and Rate Constants (*k*_q) for the DCA-Fluorescence Quenching with **1** in Various Solvents

solvent	<i>E</i> ^{ox} _{1/2} (1)/V	ΔG_{et} /eV			<i>k</i> _q /10 ¹⁰ M ^{−1} s ^{−1}
		DCA	TCNB	NMQ ⁺ BF ₄ [−]	
CH ₃ CN	+1.35	−0.61	−1.72	−1.32	1.6
CH ₂ Cl ₂	+1.53	−0.68	−1.93	−1.67	1.2
C ₆ H ₆	^c				0.9

^a In CH₃CN containing 0.1 M Et₄N⁺ClO₄[−] or in CH₂Cl₂ containing 0.1 M *n*-Bu₄N⁺ClO₄[−]. ^b $\Delta G_{\text{et}} = E^{\text{ox}}_{1/2}(\text{I}) - E^{\text{red}}_{1/2}(\text{Sens}) - E_{0-0}(\text{Sens}) - e^2/\epsilon r$. *E*^{red}_{1/2}(DCA) is −0.95 and −0.89 V vs SCE and *E*₀₋₀(DCA) is 2.91 and 2.87 eV in CH₃CN and CH₂Cl₂, respectively. *E*^{red}_{1/2}(TCNB) is −0.73 and −0.57 V vs SCE and *E*₀₋₀(TCNB) is 3.80 and 3.80 eV in CH₃CN and CH₂Cl₂, respectively. *E*^{red}_{1/2}(NMQ⁺BF₄[−]) is −0.80 and −0.51 V vs SCE and *E*₀₋₀(NMQ⁺BF₄[−]) is 3.47 and 3.48 eV in CH₃CN and CH₂Cl₂, respectively. The coulomb term (*e*²/ε*r*) is disregarded in CH₃CN and is 0.23 eV in CH₂Cl₂. ^c No attempt.

The oxidation potential (*E*^{ox}_{1/2}) of **1** (+1.35 V vs SCE in acetonitrile) is low enough to quench the excited singlet DCA, TCNB, and NMQ⁺BF₄[−] in acetonitrile, dichloromethane, or benzene by electron transfer as suggested by the calculated free energy changes (ΔG_{et}) and the observed quenching rate constants (*k*_q) shown in Table 1. In fact, as shown in Table 2, the DCA-sensitized photoreactions of *d*₂-**1** in acetonitrile, dichloromethane, and benzene under nitrogen occur in excellent yields via the degenerate rearrangement, giving rise to a near 57:43⁹ photostationary mixture of *d*₂-**1** and *d*₂-**1'**. Similar photoreaction of **1** under oxygen gives 3,3-bis(4-methoxyphenyl)-4-methylene-1,2-dioxolane (**8**)^{2,10} quantitatively as a major product in acetonitrile or dichloromethane, but in a poor yield in the less polar solvent benzene. The TCNB-sensitized photoreactions in acetonitrile give similar results, though oxygenation in dichloromethane is less efficient. In contrast, the degenerate rearrangement of *d*₂-**1** with NMQ⁺BF₄[−] and toluene (TOL, as a cosensitizer) in acetonitrile is extremely slow, while oxygenation proceeds rapidly to form **8** quantitatively. From those experimental results, it is conceivable that an immediate precursor for the degenerate rearrangement may be different from one captured by oxygen to form **8**. Under those sensitized conditions, TR absorption spectroscopy on laser flash photolysis of **1** was performed as described later.

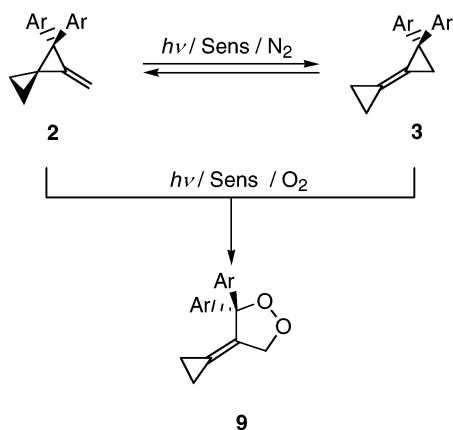
- (4) Miyashi, T.; Takahashi, Y.; Kamata, M.; Yokogawa, K.; Ohaku, H.; Mukai, T. *Phys. Org. Chem. 1986, Stud. Org. Chem.* **1986**, *31*, 363–368.
 (5) Miyashi, T.; Takahashi, Y.; Ohaku, H.; Ikeda, H.; Morishima, S.-i. *Pure Appl. Chem.* **1991**, *63*, 223–230.
 (6) Ikeda, H.; Nakamura, T.; Miyashi, T.; Goodman, J. L.; Akiyama, K.; Tero-Kubota, S.; Houmam, A.; Wayner, D. D. M. *J. Am. Chem. Soc.* **1998**, *120*, 5832–5833.
 (7) Miyashi, T.; Takahashi, Y.; Mukai, T.; Roth, H. D.; Schilling, M. L. M. *J. Am. Chem. Soc.* **1985**, *107*, 1079–1080.
 (8) The use of TCNB and NMQ⁺BF₄[−] makes it easy to observe TR absorption spectra at the region below 450 nm, while the lifetime of cation radicals is extended by coexistence of BP with DCA.

- (9) The ratio seems to be affected by the kinetic isotope effects on the CRCL and DRCY step. Similar kinetic isotope effects have been found to be responsible for the 52:48 ratio observed in the PET degenerate Cope rearrangement between 3,3,4,4-tetradeuterio-2,5-diphenyl-1,5-hexadiene and the corresponding 1,1,2,2-tetradeuterio derivative which proceeds in a cation radical cyclization–diradical cleavage mechanism.¹
 (10) (a) Miyashi, T.; Kamata, M.; Mukai, T. *J. Am. Chem. Soc.* **1986**, *108*, 2755–2757. (b) Miyashi, T.; Kamata, M.; Mukai, T. *J. Am. Chem. Soc.* **1987**, *109*, 2780–2788.

Table 2. Photostationary Ratios (d_2 -1: d_2 -1') in the Degenerate Methylene cyclopropane Rearrangement of d_2 -1, Yields of **8** in the Photooxygenation of **1**, and Transient Absorption Maxima (λ_{\max}^{500} and λ_{\max}^{350}) around 500 and 350 nm Observed in Laser Flash Photolyses of **1** under Various PET Conditions

conditions	rearrangement ^a		photooxygenation ^b		transient absorption ^c		
	time/h	d_2 -1: d_2 -1'	time/min	yield of 8 /%	λ_{\max}^{500} /nm	λ_{\max}^{350} /nm	$\Delta OD^{500}/\Delta OD^{350}$ ^d
DCA/CH ₃ CN	4.5 ^e	58:42	15	100	f	g	
DCA/CH ₂ Cl ₂	2	56:44	15	19	f	g	
DCA/C ₆ H ₆	3	57:43	120	3	f	g	
DCA-BP/CH ₃ CN	slow ^e		15	100	494	g	
TCNB/CH ₃ CN	4.5 ^e	54:46	20	100	500	351	1.3
TCNB/CH ₂ Cl ₂	3	56:44	30	4	f	354	~0
TCNB-BP/CH ₂ Cl ₂	15	56:44	15	96	508	354	2
NMQ ⁺ BF ₄ ⁻ /CH ₃ CN	slow ^e		15	100	500	352	3.6
NMQ ⁺ BF ₄ ⁻ -TOL/CH ₃ CN	slow ^e		5	100	498	350	>10

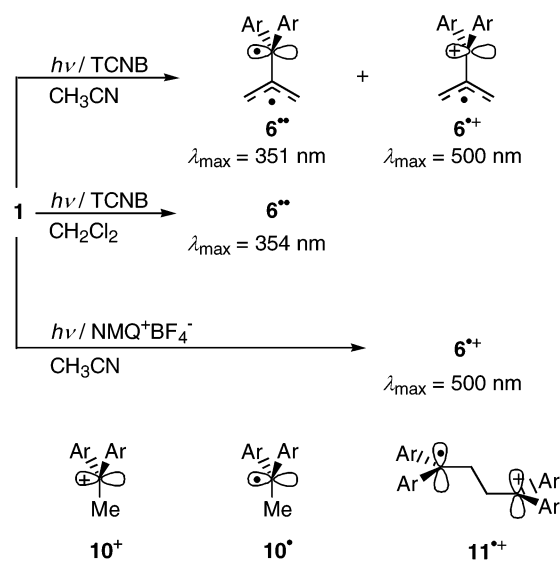
^a Under N₂. [d_2 -1] = 0.1 M in deuterated solvents. ^b Under O₂. [1] = 0.01 M. ^c Under N₂ or Ar. [1] = 0.001 M. ^d Ratio of optical density (ΔOD) of transient absorption at λ_{\max}^{500} to that at λ_{\max}^{350} at 200 ns after excitation. ^e In degassed CH₃CN. ^f No transient absorption was observed. ^g Not observable under the conditions employed.

Scheme 3. Methylene cyclopropane Rearrangement and Oxygenation of **2** and **3** Triggered by PET^a

^a Sens: DCA, TCNB, or NMQ⁺BF₄⁻.

The reversible methylene cyclopropane rearrangement of **2** and **3** is also triggered by PET. The DCA-sensitized photoreaction of **2** in acetonitrile gives a 40:60 photostationary mixture of **2** and **3** under nitrogen and gives 4-cyclopropylidene-3,3-bis(4-methoxyphenyl)-1,2-dioxolane (**9**)^{4,5} under oxygen (Scheme 3). The similarity in the reactivities of **1**, **2**, and **3** under PET conditions suggests that **1**, **2**, and **3** undergo rearrangement in a similar reaction sequence.

TR Absorption Spectroscopy on Laser Flash Photolyses of 1, 2, and 3. In an effort to characterize the proposed TMM intermediates in the rearrangements and oxygenations of **1**, **2**, and **3**, nanosecond TR absorption spectroscopy on laser flash photolysis was performed with DCA, TCNB, or NMQ⁺BF₄⁻ as a sensitizer. The spectrum obtained on laser flash photolysis of **1** with DCA in acetonitrile exhibits no clear transient absorption band, but that of **1** with DCA and biphenyl (BP, as a cosensitizer) exhibits a transient with λ_{\max} at 494 nm in acetonitrile. Since the region below 400 nm is not transparent in the DCA-sensitized reactions, relevant results were obtained with TCNB or NMQ⁺BF₄⁻ (Scheme 4). As shown in Figure 1a, laser excitation (308 nm) of TCNB with **1** in acetonitrile gives two transient absorption bands with λ_{\max} at 500 and 351 nm, showing the ratio of optical densities $\Delta OD^{500}/\Delta OD^{350} = 1.3$, whereas only the intense 350 nm transient is observed in dichloromethane (Figure 1b). The 500 nm transient corresponds to the 494 nm transient. On the other hand, when NMQ⁺BF₄⁻

Scheme 4. Assignment of the Transients Observed by TR Absorption Spectroscopy on Laser Flash Photolyses of **1** under Various PET Conditions

is used as a sensitizer in acetonitrile, the 500 nm transient is predominant with the large $\Delta OD^{500}/\Delta OD^{350}$ (Figure 1c).

The observed experimental and spectroscopic results shown in Table 2 provide a mechanistic clue to the assignment of the 500 and 350 nm transients. In the TCNB-sensitized reactions in dichloromethane where the 350 nm transient is predominant, rearrangement occurs efficiently but oxygenation does not. In contrast, in the NMQ⁺BF₄⁻-TOL-cosensitized reactions where the 500 nm transient is predominant, oxygenation occurs rapidly, while rearrangement is extremely slow. These facts reasonably suggest that the 500 and 350 nm transients are the immediate precursors, respectively, for oxygenation and rearrangement. In fact, both oxygenation and rearrangement occur efficiently with TCNB in acetonitrile, where both the 500 and 350 nm transients are observed as shown in Figure 1a.

The identities of the 500 and 350 nm transients may be inferred from λ_{\max} of 1,1-bis(4-methoxyphenyl)ethyl cation **10**⁺ (484 nm in acetonitrile and 499 nm in dichloromethane¹¹), the corresponding radical **10**[•] (349 nm in acetonitrile and 352 nm in dichloromethane), and 1,1,4,4-tetrakis(4-methoxyphenyl)-butane-1,4-diyl cation radical **11**^{•+} (500 and 350 nm in 1,2-

(11) Heublein, G.; Helbig, M. *Tetrahedron* **1974**, *30*, 2533–2536.

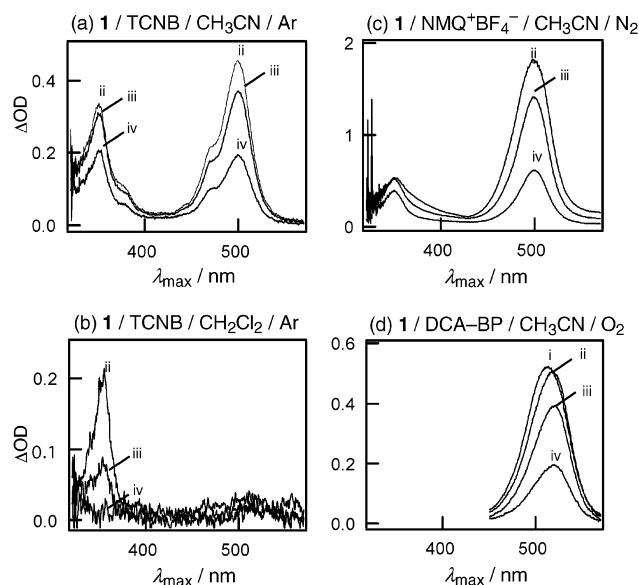
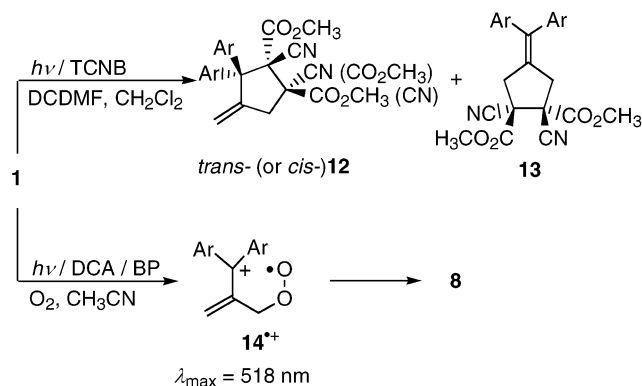


Figure 1. TR absorption spectra observed at a delay time of 60 ns (i), 200 ns (ii), 1 μ s (iii), and 5 μ s (iv) after the laser flash photolyses (308 nm excitation for TCNB and $\text{NMQ}^+\text{BF}_4^-$, 355 nm excitation for DCA) of **1** under various PET conditions.

dichloroethane, 490 and 340 nm in acetonitrile¹²). Therefore, we assign λ_{max} at 500 and 350 nm to the 1,1-bis(4-methoxyphenyl)ethyl cation moiety of the largely twisted TMM cation radical $6^{+\bullet}$ and the 1,1-bis(4-methoxyphenyl)ethyl radical moiety of the largely twisted TMM diradical $6^{\bullet\bullet}$, respectively. The most reasonable process to form $6^{\bullet\bullet}$ is back electron transfer from a sensitizer anion radical to $6^{+\bullet}$ via a contact or solvent-separated ion radical pair [$6^{+\bullet}/\text{Sens}^{\bullet-}$]. Back electron transfer from $\text{TCNB}^{\bullet-}$ to $6^{+\bullet}$ proceeds in dichloromethane much more efficiently than in polar acetonitrile, while that from NMQ^{\bullet} to $6^{+\bullet}$ must be inefficient because of the ready cage-escape of NMQ^{\bullet} and $6^{+\bullet}$. The cage-escaped $6^{+\bullet}$ is then efficiently captured by oxygen.

The decay kinetics of the 500 and 350 nm transients support their assignment to $6^{+\bullet}$ and $6^{\bullet\bullet}$. The 500 nm transient observed with DCA and BP persists for several microseconds under nitrogen in acetonitrile, but disappears completely within 200 ns under oxygen, whereby a new transient absorption band with λ_{max} at 518 nm arises, as shown in Figure 1d. This transient is presumably due to the peroxide cation radical $14^{+\bullet}$, leading to **8**. The 350 nm transient observed with TCNB in dichloromethane decays with the first-order rate constant $k = 1.1 \times 10^5 \text{ s}^{-1}$ at 20 $^\circ\text{C}$ in the absence of a trapping reagent, whereas it decays with the second-order rate constant $k = 5.2 \times 10^6 \text{ M}^{-1} \text{ s}^{-1}$ in the presence of dicyanodimethylfumarate (DCDMF), indicating chemical capture of $6^{\bullet\bullet}$ by DCDMF. In fact, under those sensitized conditions the [3 + 2] cycloadducts, *trans*- and *cis*-1,2-dicarbomethoxy-1,2-dicyano-3,3-bis(4-methoxyphenyl)-4-methylenecyclopentane (*trans*-**12**, *cis*-**12**) and *trans*-1,2-dicarbomethoxy-1,2-dicyano-4-(bis(4-methoxyphenyl)methylene)-cyclopentane (**13**), are formed in 23, 23, and 46% yields, respectively, in dichloromethane (Scheme 5). Fast and slow decay profiles of the 500 and 350 nm transient, respectively, shown in Figure 1a, are not inconsistent with the conclusion

Scheme 5. PET Reactions of **1** in the Presence of DCDMF or O_2



that $6^{\bullet\bullet}$ with λ_{max} at 350 nm is formed from $6^{+\bullet}$ with λ_{max} at 500 nm by back electron transfer. Although a kinetic analysis of the rate of back electron transfer is not successful, clean first-order kinetics is obtained for the decay of the 350 nm transient observed with TCNB as a sensitizer in dichloromethane. The temperature dependence of the first-order rate constants measured at six points between 266.7 and 299.5 K provides the Arrhenius parameters $E_a = 2.9 \text{ kcal/mol}$ and $A = 10^{7.2} \text{ s}^{-1}$. These values can be ascribed to the activation parameters for cyclization of $6^{\bullet\bullet}$ to **1**.

Transient spectra observed in the TCNB-sensitized laser flash photolyses of **2** and **3** in acetonitrile are shown in Figure 2a,b. Transient spectra from **2** and **3** bear close resemblance, indicating the generation of a similar transient species from **2** and **3**. By comparison with λ_{max} of $6^{+\bullet}$ and $6^{\bullet\bullet}$, the transient absorption bands at 500 and 350 nm are assigned to TMM cation radical $7^{+\bullet}$ and diradical $7^{\bullet\bullet}$, respectively (Scheme 6). The effects of solvent and sensitizer on the generation of the transient species from **2** and **3** are similar to those observed from **1**. Thus, the TCNB-sensitized laser flash photolyses of **2** and **3** in dichloromethane give only the 350 nm transient as shown in Figure 2c,d, whereas the intense 500 nm transient is predominant with $\text{NMQ}^+\text{BF}_4^-$ and TOL in acetonitrile as shown in Figure 2e. Therefore, it is evident that two different types of TMM intermediates participate in the singlet-sensitized electron-transfer photoreactions of **1**, **2**, and **3** as shown in Scheme 1.

EPR Spectroscopy for PET Reactions of 1–5. (1) **TR-EPR for 1–3: Evidence for the Formation of Twisted TMM Cation Radicals.** Methylenecyclopropanes **1**, **2**, and **3** were subjected to EPR spectroscopic studies to help determine the structures of TMM cation radical intermediates.¹⁴ Figure 3a shows the CIDEP spectrum observed at delay time of 1 μ s after pulsed 355 nm irradiation of a DMSO solution of **1** and CA at ambient temperatures. The E^*/E spectrum is easily reproduced by the superposition of triplet (E) and radical pair (E/A)¹⁶ signals as shown in Figure 3b, where E^* , E , and A denote excess emission, emission, and enhanced absorption of the microwave radiation, respectively. The intense signal peak at 343.135 mT ($g = 2.0058$) is assigned to $\text{CA}^{\bullet+}$. The well-separated five lines are analyzed with two hyperfine splitting (hfs) constants ($\alpha_H = 1.438$ and 1.380 mT) corresponding to $6^{+\bullet}$ ($g = 2.0031$)

(14) For an EPR spectrum of the parent TMM cation radical, see ref 15.

(15) Komaguchi, K.; Shiotani, M.; Lund, A. *Chem. Phys. Lett.* **1997**, 265, 217–223.

(16) McLauchlan, K. A. In *Modern Pulsed and Continuous-Wave Electron Spin Resonance*; Keva, L., Bowman, M. K., Ed.; Wiley: New York, 1990; pp 285–363.

(12) Fujita, M.; Shindo, A.; Ishida, A.; Majima, T.; Takamuku, S.; Fukuzumi, S. *Bull. Chem. Soc. Jpn.* **1996**, 69, 743–749.

(13) For the mechanism of the [3 + 2] cycloadditions of **1**, see ref 10.

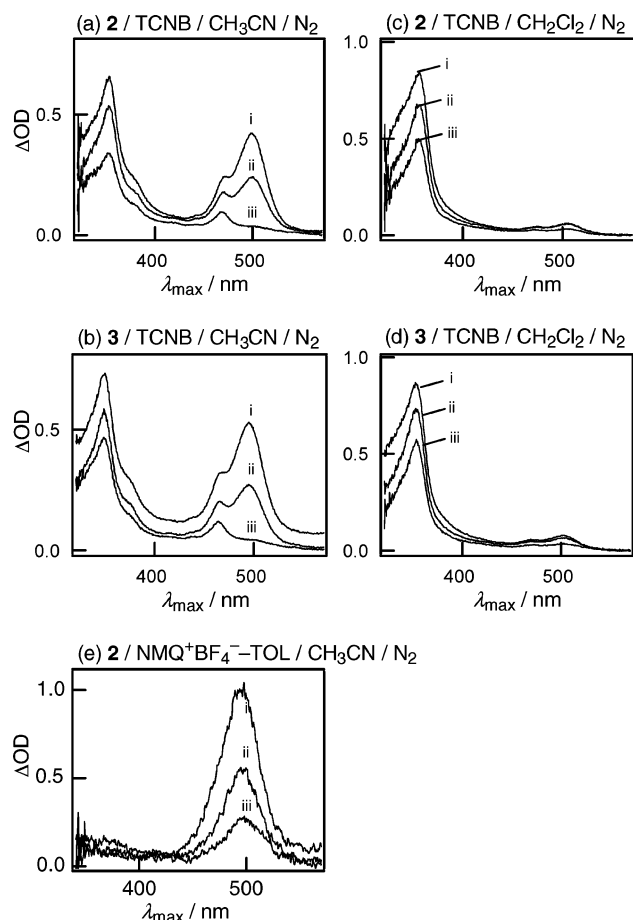
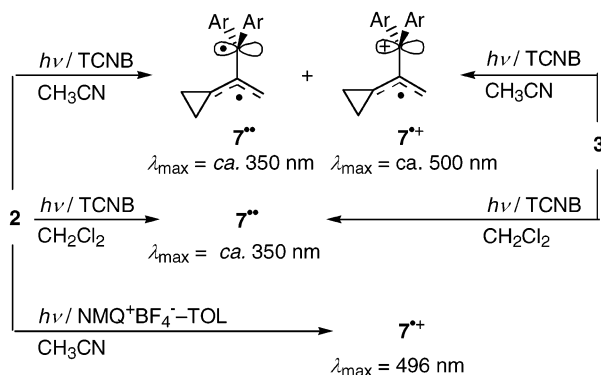


Figure 2. TR absorption spectra observed at a delay time of 200 ns (i), 1 μ s (ii), and 5 μ s (iii) after the laser flash photolyses (308 nm excitation) of **2** and **3** under various PET conditions.

Scheme 6. Assignment of the Transients Observed by TR Absorption Spectroscopy on Laser Flash Photolyses of **2** and **3** under Various PET Conditions



(Scheme 7). The contribution from the 1,1-bis(4-methoxyphenyl)ethyl moiety to the spectrum is in the range of the line width, indicating a negligibly small population of the unpaired electron in this moiety. Since the hfs constants and the g -value are close to those of the parent allyl radical,^{17,19} the unpaired electron must be located mainly on the allyl moiety of **6**^{•+}, indicating its largely twisted structure. This conclusion is thus consistent

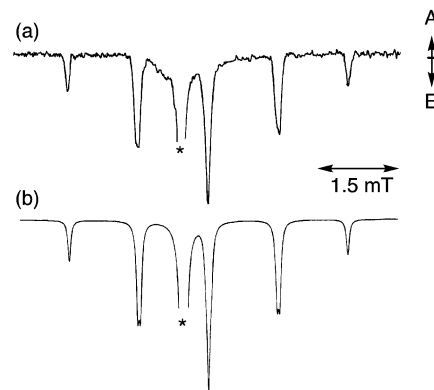
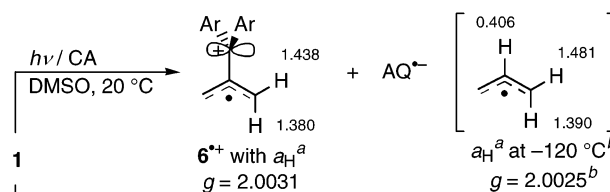


Figure 3. CIDEP spectrum of **6**^{•+} observed at a delay time of 1 μ s after the laser excitation (355 nm) of CA (10 mM) with **1** (50 mM) in DMSO at ambient temperature (a) and its simulation with the parameters given in Scheme 7 (b). Asterisks (*) represent emissions due to CA^{•-}.

Scheme 7. Assignment of the Transients Observed by TR-EPR on Laser Flash Photolyses of **1** under Various PET Conditions



^a In mT. ^b See ref 17.

with a previous proposal based on the CIDNP experiments by Miyashi, Roth, and co-workers.⁷

The CIDEP spectrum of **7**^{•+} is similarly obtained on laser excitation (355 nm) of a propylene carbonate (PC) solution of CA and **2** or **3** at ambient temperatures (Figure 4, Scheme 8). As expected from TR absorption spectroscopy on laser flash photolysis of **2** and **3**, the CIDEP spectrum from **2** nearly coincides with that from **3**, showing slight differences in the contribution ratio of triplet (E) and radical pair (E/A) mechanisms as shown in Figure 4a–c.

(2) TR-EPR for 4, Z-5, and E-5: Stereochemistry for the Formation of Twisted TMM Cation Radicals at the CRCL Step. Recent calculations of Cramer and Smith²¹ have shown that in the parent TMM the planar structure is more stable than the bisected one by ca. 14 kcal/mol. Nevertheless, the dianisyl-substituted TMM diradicals **6**^{••} and **7**^{••} are twisted largely. Because their cation radical precursors **6**^{•+} and **7**^{•+} are also the largely twisted species, the stereochemistry of cleavage at the CRCL step is most responsible for the formation of the twisted structures of **6**^{••} and **7**^{••}. As a previous CIDNP study⁷ proposed, the less bulky C-3 methylene group of **1**^{•+} preferentially rotates to form **6**^{•+} in the least motion pathway, keeping the σ -orbital of the C-1 dianisylmethylene group orthogonal to the methylene π -system as shown in Scheme 1. Probably, the double rotation at C-1 and C-3 would cause significant steric destabilization of the resulting planar TMM cation radical. To gain further insight into the stereochemistry of cleavage at the CRCL step, we investigated the CA-sensitized photoreactions of the monoanisyl derivatives 2-(4-methoxyphenyl)-1-methylenecyclopropane (**4**), Z-5, and E-5 by TR-EPR.

(17) Krusic, P. J.; Meakin, P.; Smart, B. E. *J. Am. Chem. Soc.* **1974**, *96*, 6211–6213. See also ref 18.

(18) Fessenden, R. W.; Schuler, R. H. *J. Chem. Phys.* **1963**, *39*, 2147–2195.

(19) See also the data of 2-methylallyl radical²⁰ shown in Scheme 9.

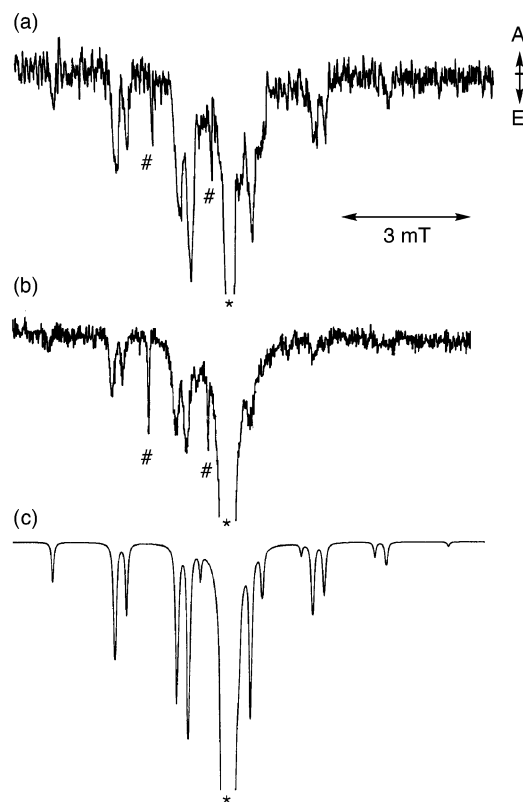
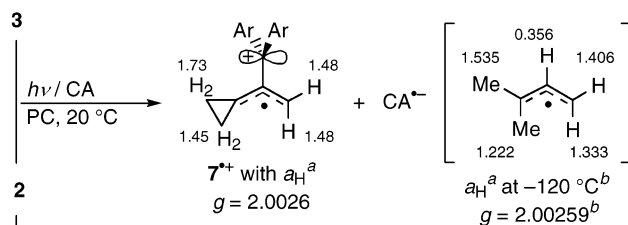


Figure 4. CIDEP spectra of 7^{*+} observed at a delay time of 500 ns after the laser excitation (355 nm) of CA (5 mM) with **2** (10 mM) (a) and of CA (20 mM) with **3** (20 mM) (b) in PC under Ar at ambient temperature and its simulation with the parameters given in Scheme 8 (c). Asterisks (*) and pound signs (#) represent emissions due to CA^{*+} and a radical species derived from PC, respectively.

Scheme 8. Assignment of the Transients Observed by TR-EPR on Laser Flash Photolyses of **2** and **3** under Various PET Conditions



^a In mT. ^b See ref 17.

Figure 5a shows a CIDEP spectrum obtained on laser excitation of CA with **4** in DMSO at ambient temperatures. The structure of 15^{*+} is confirmed by three hfs constants shown in Scheme 9 obtained from the hyperfine structure and spectral simulation shown in Figure 5b. Similar CIDEP spectra obtained by stereoselective cleavage of $Z\text{-}5^{*+}$ and $E\text{-}5^{*+}$ are shown in Figure 5 together with simulated spectra. The structures of $Z\text{-}16^{*+}$ and $E\text{-}16^{*+}$ are similarly determined by comparison of their hfs constants with those of (*Z*)- and (*E*)-1-methylallyl radicals²⁰ shown in Scheme 9. Apparently, the unpaired electrons in 15^{*+} , $Z\text{-}16^{*+}$, and $E\text{-}16^{*+}$ are localized predominantly on the allyl or methylallyl radical moiety. However, very small hfs

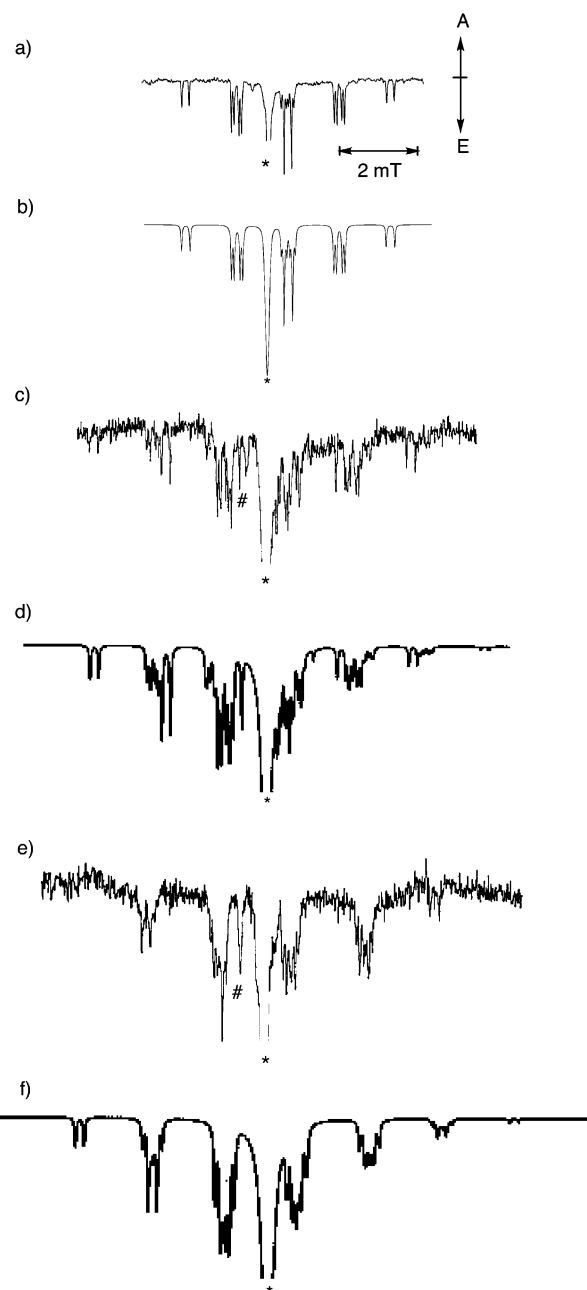


Figure 5. CIDEP spectra of 15^{*+} (a), $Z\text{-}16^{*+}$ (c), and $E\text{-}16^{*+}$ (e) observed at a delay time of 500 ns after the laser excitation (355 nm) of CA (20 mM) with **4** (10 mM), **Z-5**, and **E-5**, respectively, in DMSO under Ar at ambient temperature and simulated spectra of 15^{*+} (b), $Z\text{-}16^{*+}$ (d), and $E\text{-}16^{*+}$ (f) with the parameters given in Scheme 9. Asterisks (*) and pound signs (#) represent emissions due to CA^{*+} and a radical species (probably $CH_3SOCH_2^{\bullet}$) derived from DMSO, respectively.

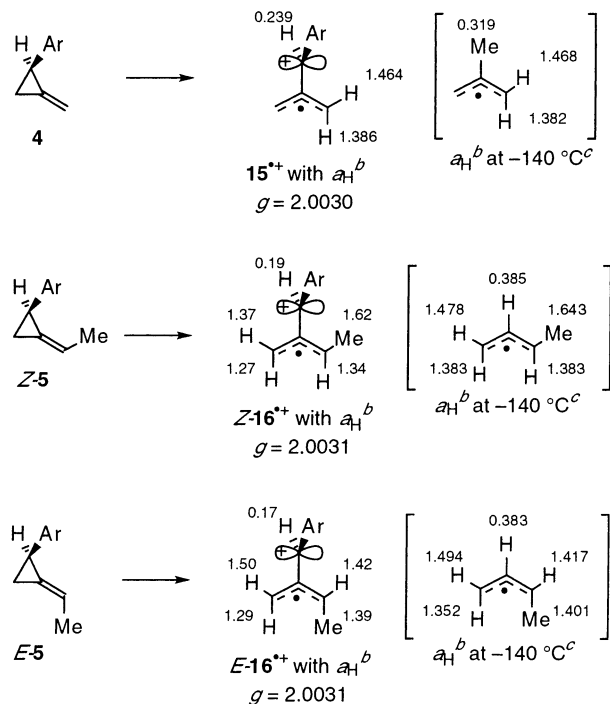
constants are observed for the hydrogen (H_{C-2} in Scheme 10) on the carbon bearing the anisyl group in 15^{*+} , $Z\text{-}16^{*+}$, and $E\text{-}16^{*+}$.

On the assumption that the hfs of H_{C-2} of 15^{*+} originates mainly from spin density at C-1 of the allyl radical part as does that of 2-methylallyl, the dihedral angle (θ in Scheme 10) between two planes of the allyl radical moiety and the $Ar-C^+-H$ moiety in 15^{*+} is estimated using the following equation:²³ $a_H(H_{C-2}) = [B_0 + B_2 \cos^2(90 - \theta)]\rho(C-1)$, where $a_H(H_{C-2})$, B_0

(20) Kochi, J. K.; Krusic, P. J. *J. Am. Chem. Soc.* **1968**, *90*, 7157–7159.

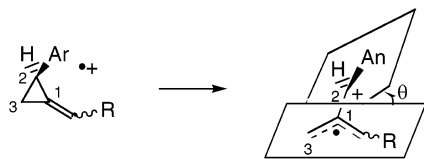
(21) Cramer, C. J.; Smith, B. A. *J. Phys. Chem.* **1996**, *100*, 9664–9670. See also ref 22.

Scheme 9. Assignment of the Transients Observed by TR-EPR on Laser Flash Photolyses of **4**, **Z-5**, and **E-5** under PET Conditions



^a Conditions; $h\nu$ /CA, DMSO, 20 °C. ^bIn mT. ^cSee ref 20.

Scheme 10. Numbering and Definition of θ in **15^{•+}**, **Z-16^{•+}**, and **E-16^{•+}**



and B_2 , and $\rho(\text{C-1})$ are the hfs constant of $\text{H}_{\text{C-2}}$, constant terms, and spin density of C-1, respectively. When the spin polarization effects are very small for $\text{H}_{\text{C-2}}$, the value B_0 can be disregarded. The value $B_2\rho(\text{C-1}) = 0.638\text{ mT}$ is obtained from the hfs constant for the methyl proton of the 2-methylallyl radical [$a_{\text{H}}(\text{CH}_3) = 0.319\text{ mT}$],²⁰ in which $\cos^2(90 - \theta) \approx \langle \cos^2(90 - \theta) \rangle = 0.5$, assuming free rotation of the methyl group of the 2-methylallyl radical.²⁴ Using the estimated value $B_2\rho(\text{C-1}) = 0.638\text{ mT}$ and experimental value $a_{\text{H}}(\text{H}_{\text{C-2}}) = 0.239\text{ mT}$, θ in **15^{•+}** is calculated to be 38° . Since the $\text{Ar-C}^+-\text{H}$ group in **15^{•+}** is less bulky than the $\text{Ar-C}^+-\text{Ar}$ group in **6^{•+}**, θ of **15^{•+}** must be reduced as compared with that of **6^{•+}**. In fact, a preliminary calculation using AM1 UHF parameters²⁵ suggests that θ of **6^{•+}** and **15^{•+}** are ca. 44° and 24° , respectively. Nevertheless, the unpaired electrons in **Z-16^{•+}** and **E-16^{•+}** are localized predominantly on the methylallyl radical moiety. Note that they are formed respectively from **Z-5^{•+}** and **E-5^{•+}** by rotating the less bulky C-3 methylene groups and keeping intact the relative

Table 3. ZFS Values of **6^{••}**, **7^{••}**, and the Parent TMM Diradical

	$ D/hc /\text{cm}^{-1}$	$ E/hc /\text{cm}^{-1}$
6^{••}	0.0116	0.0038
7^{••}	0.012	0.0039
parent TMM ^a	0.024	0

^a See ref 27.

orientation of the anisyl and methyl groups. Probably, a potential rotation of the anisylmethylene group of **4^{•+}**, **Z-5^{•+}**, and **E-5^{•+}** and of the dianisylmethylene group of **1^{•+}**, **2^{•+}**, and **3^{•+}** would induce steric compression and thereby inhibit the formation of planar TMM cation radical intermediates.

(3) Steady State (SS)-EPR for 1–3: Observation of the Twisted TMM Generated in the PET Reactions. For the spectroscopic identification of diradicals **6^{••}** and **7^{••}** from **1** and **2**, the SS-EPR measurements were performed at cryogenic temperature. Upon the pulsed 355 nm irradiation of AQ with **1** in a dichloromethane matrix at 22 K, a characteristic EPR spectrum of a randomly oriented triplet species ascribed to **6^{••}** is observed together with a signal due to **6^{•+}**. In addition to the $|\Delta M_s| = 1$ transition signals, a weak $|\Delta M_s| = 2$ transition is observed at 167.3 mT. The triplet signal of **6^{••}** persists at cryogenic temperature, and the Curie plot²⁶ of the $|\Delta M_s| = 2$ transition signal intensities gives a straight line between 4.2 and 40 K, indicating the triplet ground state of **6^{••}** as the usual TMM diradical derivatives. The AQ-sensitized photoreaction of **2** gives a similar EPR spectrum with a $|\Delta M_s| = 2$ transition at 167.5 mT, which is ascribed to **7^{••}**.

As shown in Table 3, the zero-field splitting (ZFS) parameters of **6^{••}** and **7^{••}** are characterized by relatively small $|D/hc|$ and large $|E/hc|$ values as compared with those of the parent planar TMM diradical.²⁷ Small $|D/hc|$ values may reflect the nonplanar structures of **6^{••}** and **7^{••}**. The deduction of the $|D/hc|$ values caused by the deviation from planar conformation has been reported for a series of biphenyl derivatives,²⁸ conjugated enones,²⁹ and conjugated TMM diradical derivatives.³⁰

The most likely process to form **6^{••}** and **7^{••}** is back electron transfer from a sensitizer anion radical to **6^{•+}** and **7^{•+}** without structural change, respectively. Taking account of the fact that TR absorption spectra of **6^{••}** and **7^{••}** are coincident with that of **10[•]**, it is reasonable to conclude that both **6^{••}** and **7^{••}** are also twisted. Consequently, small $|D/hc|$ values of **6^{••}** and **7^{••}** are consistent with their large $|E/hc|$ values which are related to the molecular symmetry. EPR spectroscopic results clearly indicate that two different types of TMM intermediates are formed also in the triplet-sensitized electron-transfer photoreactions of **1**, **2**, and **3**.

Mechanism of the Degenerate Methylenecyclopropane Rearrangement Based on Energetics. (1) Determination of the Energy of $[\text{6}^{\bullet+}/\text{DCA}^{\bullet-}]$ by Photoacoustic Calorimetry. A reasonable mechanism to explain the spectroscopic detection of **6^{••}** and **6^{•+}** is a cation radical cleavage (CRCL)–diradical cyclization (DRCY) mechanism shown in Scheme 1a. In this

- (22) (a) Davidson, E. R.; Borden, W. T. *J. Am. Chem. Soc.* **1977**, *99*, 2053–2060. (b) Davis, J. H.; Goddard, W. A., III. *J. Am. Chem. Soc.* **1977**, *99*, 4242–4247.
 (23) Heller, C.; McConnell, H. M. *J. Chem. Phys.* **1960**, *32*, 1535–1539.
 (24) A PM3 UHF calculation suggests that there is no significant activation energy for free rotation of the methyl group in the 2-methylallyl radical. See also ref 25.
 (25) A preliminary semiempirical calculation was carried out using MOPAC ver. 6 on a CAChe WorkSystem.

- (26) A figure of the Curie plot for **6^{••}** is available as Supporting Information in ref 6.
 (27) (a) Dowd, P. *J. Am. Chem. Soc.* **1966**, *88*, 2587–2589. (b) Dowd, P. *Acc. Chem. Res.* **1972**, *5*, 242–248. (c) Dixon, D. A.; Dunning, T. H., Jr.; Eades, R. A.; Kleier, D. A. *J. Am. Chem. Soc.* **1981**, *103*, 2878–2880.
 (28) Tanigaki, K.; Taguchi, N.; Yagi, M.; Higuchi, J. *Bull. Chem. Soc. Jpn.* **1989**, *62*, 668–673.
 (29) Yamauchi, S.; Hirota, N.; Higuchi, J. *J. Phys. Chem.* **1988**, *92*, 2129–2133.
 (30) Bushby, R. J.; Jarecki, C. *Tetrahedron Lett.* **1986**, *27*, 2053–2056.

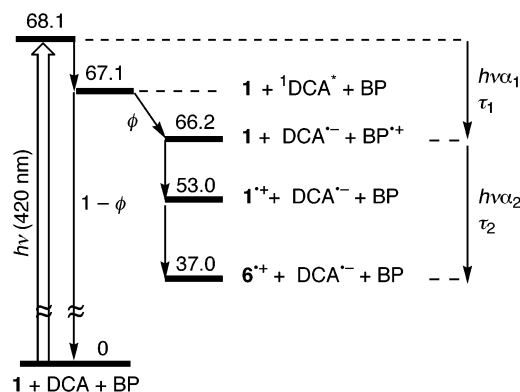


Figure 6. Schematic diagram of photoacoustic calorimetry for the 1/DCA-BP system. Relative energy is represented in kcal/mol. The value, 37.0 kcal/mol, is obtained using eq 1. For other values, see text and footnote 39.

mechanism, cation radical $d_2\text{-}6^{+\bullet}$ is formed from $d_2\text{-}1^{+\bullet}$ and $d_2\text{-}1'^{+\bullet}$ in the CRCL step and cyclization of diradical $d_2\text{-}6^{+\bullet}$ regenerates $d_2\text{-}1$ and $d_2\text{-}1'$ in the DRCY step. The key process in this mechanism is thus the formation of $d_2\text{-}6^{+\bullet}$ from $d_2\text{-}6^{+\bullet}$ by back electron transfer, which will formally compete with cyclization of $d_2\text{-}6^{+\bullet}$ to regenerate $d_2\text{-}1^{+\bullet}$ and $d_2\text{-}1'^{+\bullet}$. However, this cyclization should be energetically unfavorable on the basis of the calculations of Borden³¹ and Kikuchi³² that suggest exergonic ring cleavage of methylenecyclopropane cation radicals. To investigate the relative energetics of these processes, photoacoustic calorimetry was employed.³³

Photoacoustic calorimetry is a useful technique to determine the energetics of various photoreactions, especially the enthalpy of formation of the ion radical pair (ΔH_{irp}) of PET reactions, as has been reported previously.^{1,33–36} For reasons of experimental limitation, photoacoustic calorimetry was performed for the 1/DCA-BP system in acetonitrile according to the reported procedure.^{1,33–36} Figure 6 shows a schematic diagram for the 1/DCA-BP system. Actually, the value determined by photoacoustic calorimetry under these conditions is the enthalpy of formation of free ion radicals ($6^{+\bullet} + \text{DCA}^{\bullet-}$), $\Delta H_{\text{fir}}(6^{+\bullet} + \text{DCA}^{\bullet-})$. It can be regarded, however, as $\Delta H_{\text{irp}}(6^{+\bullet}/\text{DCA}^{\bullet-})$, because energy gaps between an ion radical pair and the corresponding free ion radicals are generally quite small in acetonitrile. The $\Delta H_{\text{irp}}(6^{+\bullet}/\text{DCA}^{\bullet-})$ value can be expressed by eqs 1 and 2,³⁵ where $h\nu$, Φ , and $E([\text{BP}^{\bullet+}/\text{DCA}^{\bullet-}])$ are photon energy (420 nm, 68.1 kcal/mol), the quantum yield to form $[\text{BP}^{\bullet+}/\text{DCA}^{\bullet-}]$, and the ion radical pair energy (66.2 kcal/mol) of $[\text{BP}^{\bullet+}/\text{DCA}^{\bullet-}]$, determined from the redox potentials of BP ($E^{\text{ox}}_{1/2} = +1.92$ V vs SCE in acetonitrile) and DCA, respectively.

$$\Delta H_{\text{irp}}(6^{+\bullet}/\text{DCA}^{\bullet-}) = h\nu(1 - \alpha_1 - \alpha_2)/\Phi \quad (1)$$

$$\Phi = h\nu(1 - \alpha_1)/E([\text{BP}^{\bullet+}/\text{DCA}^{\bullet-}]) \quad (2)$$

From the deconvolution fitting parameters ($\alpha_1 = 0.27 \pm 0.03$ and $\alpha_2 = 0.28 \pm 0.04$)³⁷ obtained from several experiments,

- (31) Du, P.; Borden, W. T. *J. Am. Chem. Soc.* **1987**, *109*, 5330–5336.
 (32) Takahashi, O.; Morishashi, K.; Kikuchi, O. *Tetrahedron Lett.* **1990**, *31*, 5175–5178.
 (33) (a) Rudzki, J. E.; Goodman, J. L.; Peters, K. S. *J. Am. Chem. Soc.* **1985**, *107*, 7849–7854. (b) Herman, M. S.; Goodman, J. L. *J. Am. Chem. Soc.* **1989**, *111*, 1849–1854. (c) Griller, D.; Wayner, D. D. M. *Pure Appl. Chem.* **1989**, *61*, 717–724.
 (34) Peters, K. S. In *Kinetics and Spectroscopy of Carbenes and Biradicals*; Platz, M. S., Ed.; Plenum: New York, 1990; pp 37–49.

$\Delta H_{\text{irp}}(6^{+\bullet}/\text{DCA}^{\bullet-})$ is determined to be 37.0 ± 0.8 kcal/mol.³⁸ Since the free energy change for the formation of $[1^{+\bullet}/\text{DCA}^{\bullet-}]$ is 53 kcal/mol,³⁹ the ion radical pair $[6^{+\bullet}/\text{DCA}^{\bullet-}]$ lies 16 kcal/mol lower in energy than $[1^{+\bullet}/\text{DCA}^{\bullet-}]$. This is supported by an MNDO UHF calculation²⁵ which predicts that $6^{+\bullet}$ lies 18 kcal/mol lower than $1^{+\bullet}$. This suggests that cyclization of $d_2\text{-}6^{+\bullet}$ to $d_2\text{-}1^{+\bullet}$ (or $d_2\text{-}1'^{+\bullet}$) is significantly endergonic and unlikely to operate in the degenerate rearrangement of $d_2\text{-}1$.

(2) **Energetics from $[6^{+\bullet}/\text{DCA}^{\bullet-}]$.** In contrast, the back electron transfer from $\text{DCA}^{\bullet-}$ to $6^{+\bullet}$ to form $6^{+\bullet}$ is estimated to be exergonic by 21 kcal/mol, using the oxidation potential of 10^{\bullet} ($E^{\text{ox}}_{1/2} = -0.06$ V vs SCE in acetonitrile) determined by photomodulation voltammetry, on the assumption that $E^{\text{ox}}_{1/2}$ of the largely twisted $6^{+\bullet}$ is comparable with that of 10^{\bullet} . Accordingly, this electron-transfer process should take place rapidly with an estimated rate constant (k_{bet})^{40,43} of $1.0 \times 10^{10} \text{ s}^{-1}$ in acetonitrile at 20 °C. Although the ground state of $6^{+\bullet}$ is probably triplet ($^36^{+\bullet}$) as shown above, $6^{+\bullet}$ right after back electron transfer under those conditions must be singlet ($^16^{+\bullet}$) because a fast sequence of the CRCL and back electron transfer in $^1[1^{+\bullet}/\text{DCA}^{\bullet-}]$ conserves the singlet multiplicity originated in ^1DCA .⁴⁵ Diradical $^16^{+\bullet}$ is thus estimated to lie 16 kcal/mol higher in energy than **1**, as shown in Figure 7. According to the calculation of Cramer and Smith,²¹ the energy gap between the parent bisected-singlet and -triplet TMM diradicals is less than 2 kcal/mol. If the energy gap between the largely twisted $^16^{+\bullet}$ and $^36^{+\bullet}$ is also small, $^36^{+\bullet}$ will lie 15 ± 1 kcal/mol⁴⁷ higher in energy than **1** and will cyclize to **1**.

- (35) (a) Rothberg, L. J.; Simon, J. D.; Bernstein, M.; Peters, K. S. *J. Am. Chem. Soc.* **1983**, *105*, 3464–3468. (b) Goodman, J. L.; Peters, K. S. *J. Am. Chem. Soc.* **1986**, *108*, 1700–1701. (c) Ci, X.; da Silva, R. S.; Goodman, J. L.; Nicodem, D. E.; Whitten, D. G. *J. Am. Chem. Soc.* **1988**, *110*, 8548–8550. (d) Zona, T. A.; Goodman, J. L. *Tetrahedron Lett.* **1992**, *33*, 6093–6096. (e) LaVilla, J. A.; Goodman, J. L. *J. Am. Chem. Soc.* **1989**, *111*, 712–714.
 (36) Ikeda, H.; Takasaki, T.; Takahashi, Y.; Konno, A.; Matsumoto, M.; Hoshi, Y.; Aoki, T.; Suzuki, T.; Goodman, J. L.; Miyashi, T. *J. Org. Chem.* **1999**, *64*, 1640–1649.
 (37) At the same time, a parameter $\tau_2 = 237 \pm 110$ ns was obtained.
 (38) Although BP coexisted with **1** and DCA, the value of $\Delta H_{\text{irp}}(6^{+\bullet}/\text{DCA}^{\bullet-})$ can be obtained independently of BP as the free enthalpy changes between **1** + DCA + BP and $1^{+\bullet} + \text{DCA}^{\bullet-} + \text{BP}$ states.
 (39) The value, 53 kcal/mol, can be calculated using the redox potentials of **1** and DCA.
 (40) The rate constant (k_{bet}) for the back electron transfer in $[6^{+\bullet}/\text{DCA}^{\bullet-}]$ at 20 °C in acetonitrile was calculated using the following equations (3,⁴¹ 4,⁴¹ and 5) and parameters reported by Kikuchi and co-workers.⁴²

$$k_{\text{bet}} = \left(\frac{4\pi^3}{h^2 \lambda_s k_b T} \right)^{1/2} |V|^2 \sum_{w=0}^{\infty} \left(\frac{e^{-s} s^w}{w!} \right) \exp \left\{ - \frac{(\lambda_s + \Delta G_{\text{bet}} + w h \nu)^2}{4 \lambda_s k_b T} \right\} \quad (3)$$

$$S = \lambda_s / h \nu \quad (4)$$

$$\Delta G_{\text{bet}}(\text{eV}) = -[E^{\text{ox}}_{1/2}(10^{\bullet}) - E^{\text{red}}_{1/2}(\text{DCA})] \quad (5)$$

in which parameters V , λ_s , ν , and ΔG_{bet} are, respectively, an electronic coupling matrix element (39 cm^{-1}), solvent reorganization energy (1.45 eV), vibration reorganization energy (0.3 eV), single average frequency (1500 cm^{-1}), and free energy change for electron-transfer process (−0.89 eV). In addition, h , k_b , and T are Planck's constant, Boltzmann's constant, and temperature (293 K), respectively.

- (41) (a) Miller, J. R.; Beitz, J. V.; Huddleston, R. K. *J. Am. Chem. Soc.* **1984**, *106*, 5057–5068. (b) Siders, P.; Marcus, R. A. *J. Am. Chem. Soc.* **1981**, *103*, 741–747. (c) Siders, P.; Marcus, R. A. *J. Am. Chem. Soc.* **1981**, *103*, 748–752. (d) Van Duyne, R. P.; Fischer, S. F. *Chem. Phys.* **1974**, *5*, 183–197. (e) Ulstrup, J.; Jortner, J. *J. Chem. Phys.* **1975**, *63*, 4358–4368.
 (42) Niwa, T.; Kikuchi, K.; Matsushita, N.; Hayashi, M.; Katagiri, T.; Takahashi, Y.; Miyashi, T. *J. Phys. Chem.* **1993**, *97*, 11960–11964.
 (43) If parameters by Farid and co-workers⁴⁴ are used, k_{bet} is calculated to be $3.1 \times 10^8 \text{ s}^{-1}$.
 (44) Gould, I. R.; Ege, D.; Moser, J. E.; Farid, S. *J. Am. Chem. Soc.* **1990**, *112*, 4290–4301.
 (45) No efficient intersystem crossing from $^1\text{DCA}^{\bullet}$ to $^3\text{DCA}^{\bullet}$ has been observed in acetonitrile ($\Phi_{\text{isc}} = 0.003$).⁴⁶
 (46) Hanaoka, K. Master Thesis, Tohoku University, 1991.

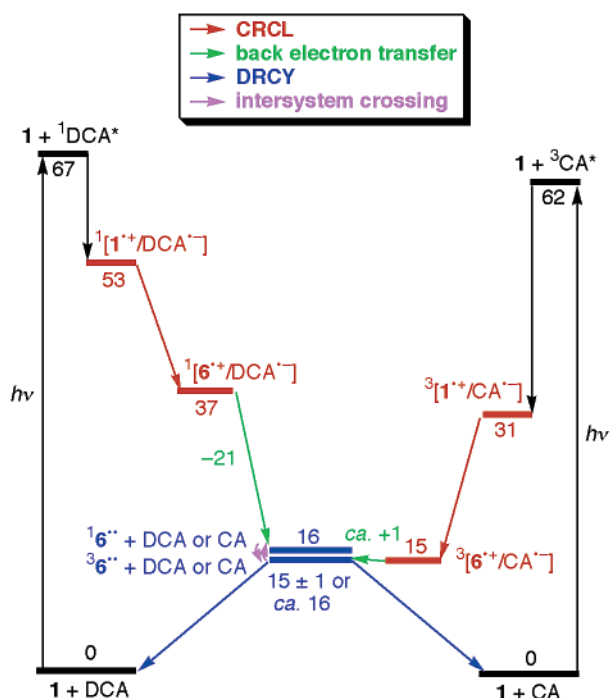


Figure 7. Energy diagram for the DCA- (left) and CA-sensitized (right) PET degenerate methylenecyclopropane rearrangement of **1** in acetonitrile. Relative energy is represented in kcal/mol. The values, 15 ± 1 and ca. 16 kcal/mol, for $^3\mathbf{6}^{\bullet\bullet}$ were obtained by analyzing the diagram of the DCA- and CA-sensitized reaction, respectively.⁴⁷

In consequence, energetics based on photoacoustic calorimetry suggests that back electron transfer to form diradical $d_2\text{-}\mathbf{6}^{\bullet\bullet}$ operates in preference to cyclization of $d_2\text{-}\mathbf{6}^{+\bullet}$, supporting a CRCL–DRCY mechanism shown in Scheme 1a. Similarities in reactivities and spectroscopic results among **1**, **2**, and **3** reasonably suggest that the reversible rearrangement between **2** and **3** proceeds with similar energetics.

(3) Common Mechanistic Channel between the DCA- and CA-Sensitized Photoreactions of 1 and Role of the Triplet TMM Diradical at the DRCY Step. Since the degenerate methylenecyclopropane rearrangement of $d_2\text{-}\mathbf{1}$ occurs in both singlet- and triplet-sensitized electron-transfer photoreactions, there must be a common mechanistic channel between these different photoreactions. A conceivable common process will be the DRCY process, in which the triplet diradical $d_2\text{-}\mathbf{3}\mathbf{6}^{\bullet\bullet}$ cyclizes to regenerate $d_2\text{-}\mathbf{1}$ and $d_2\text{-}\mathbf{1}'$. Taking account of the results of photoacoustic calorimetry of the DCA-sensitized photoreaction, plausible mechanistic relationships between the DCA- and CA-sensitized photoreactions are depicted in Figure 7. The triplet diradical $^3\mathbf{6}^{\bullet\bullet}$ can be formed also in the CA-sensitized photoreaction. The initial electron transfer from **1** to $^3\text{CA}^*$ forms $^3[1^{\bullet+}/\text{CA}^{\bullet-}]$, which is calculated to lie 31 kcal/mol higher in energy than **1** by redox potentials of CA ($E^{\text{red}}_{1/2} = 0.00$ V vs SCE in acetonitrile) and **1**. Then, the 16 kcal/mol exergonic ring cleavage of $1^{\bullet+}$ forms the triplet ion radical pair $^3[6^{\bullet+}/\text{CA}^{\bullet-}]$, which is thus estimated to lie 15 kcal/mol higher in energy than **1** (Figure 7). The cation radical species captured

by TR-EPR must be the cage-escaped $6^{\bullet+}$ from $^3[6^{\bullet+}/\text{CA}^{\bullet-}]$. The energy of $^3\mathbf{6}^{\bullet\bullet}$ formed by back electron transfer in $^3[6^{\bullet+}/\text{CA}^{\bullet-}]$ ⁴⁸ can be calculated to be ca. 16 kcal/mol because the back electron transfer is expected to be endergonic by ca. +1 kcal/mol using $E^{\text{ox}}_{1/2}(\mathbf{10}^{\bullet})$ and the reduction potential of CA.⁴⁷ Thus, the energy level of $^3\mathbf{6}^{\bullet\bullet}$ formed in this process will be nearly the same as that of $^3\mathbf{6}^{\bullet\bullet}$ formed in the DCA-sensitized photoreaction. This agreement strongly suggests that evaluation of the above energy gap between $16^{\bullet\bullet}$ and $^3\mathbf{6}^{\bullet\bullet}$ is reasonable and that the intersystem crossing between them is facile in both the DCA- and CA-sensitized photoreactions. The triplet species detected by the SS-EPR must be the resulting $^3\mathbf{6}^{\bullet\bullet}$, which rotates the methylene group while cyclizing to regenerate the singlet **1**. The Arrhenius *A* factor obtained for the decay of $6^{\bullet\bullet}$ formed in the TCNB reaction supports this possibility. The observed *A* factor ($10^{7.2} \text{ s}^{-1}$) is quite small and actually even smaller than the value, $A = 10^{9.1} \text{ s}^{-1}$, observed for the decay of the parent planar-triplet TMM diradical.⁴⁹ Unusually small *A* factors are often observed with reactions involving intersystem crossing.⁵¹ A plausible process to reproduce **1** at the DRCY step is, thus, the spin-forbidden cyclization of the triplet diradical $6^{\bullet\bullet}$ as shown in Figure 7.

Conclusion

We are the first to observe both reactive cation radical and diradical intermediates simultaneously in the same PET isomerization system. By the combination of product analysis, spectroscopy, and calorimetry, it can be concluded that the PET degenerate rearrangement of $d_2\text{-}\mathbf{1}$ proceeds in a CRCL–DRCY mechanism shown in Scheme 1a, involving the largely twisted TMM cation radical and diradical intermediates $d_2\text{-}\mathbf{6}^{+\bullet}$ and $d_2\text{-}\mathbf{6}^{\bullet\bullet}$, respectively. Cation radical $d_2\text{-}\mathbf{6}^{+\bullet}$ is formed in the least motion pathway at the CRCL step in which only the C-3 methylene group rotates but the bulkier C-1 dianisylmethylene group does not, evading stereochemical disadvantages caused by the anisyl groups in a hypothetical planar TMM cation radical. The back electron transfer from a sensitizer anion radical to $d_2\text{-}\mathbf{6}^{+\bullet}$ is the most important process in this rearrangement. Cyclization of the resulting $d_2\text{-}\mathbf{6}^{\bullet\bullet}$ completes the degenerate rearrangement, regenerating $d_2\text{-}\mathbf{1}$ and $d_2\text{-}\mathbf{1}'$ at the DRCY step. Close resemblances in reactivities and spectroscopic results among **1**, **2**, and **3** support the operation of a CRCL–DRCY mechanism in the reversible methylenecyclopropane rearrangement between **2** and **3** as shown in Scheme 1b.

Experimental Section

General Method. See the Supporting Information.

Syntheses. See the Supporting Information for details. Physical data of key compounds are as follows.

(i) 1,1-Bis(4-methoxyphenyl)-2-methylenecyclopropane (1): mp 31–32 °C (colorless prisms from *n*-hexane); ^1H NMR (200 MHz, CDCl_3) δ 1.81 (dd, $J = 2.6, 2.0$ Hz, 2 H), 3.77 (s, 6 H), 5.66 (t, $J = 2.0$ Hz, 1 H), 5.77 (d, $J = 2.6$ Hz, 1 H), 6.81 (AA'BB', $J = 8.0$ Hz, 4 H), 7.20 (AA'BB', $J = 8.0$ Hz, 4 H); MS (60 °C, 13.5 eV) m/z (relative intensity) 266 (100, M^+), 251 (41), 251 (50).

(47) To verify the relatively low energy value (15 ± 1 or ca. 16 kcal/mol) for $^3\mathbf{6}^{\bullet\bullet}$, one of the reviewers suggested comparing the energy value with the estimated value obtained using calculation results for the parent TMM. Although this estimate involves many assumptions and considerable uncertainty, it suggests that the energy of $^3\mathbf{6}^{\bullet\bullet}$ is 10–24 kcal/mol, which is not inconsistent with the value obtained for $^3\mathbf{6}^{\bullet\bullet}$ in this work. Details are given in the Supporting Information.

(48) An alternative pathway for the formation of $^3\mathbf{6}^{\bullet\bullet}$ is a sequence of (i) intersystem crossing of $^3[6^{\bullet+}/\text{CA}^{\bullet-}]$ to $^1[6^{\bullet+}/\text{CA}^{\bullet-}]$, (ii) spin-allowed back electron transfer within $^1[6^{\bullet+}/\text{CA}^{\bullet-}]$, and (iii) intersystem crossing of the resulting $16^{\bullet\bullet}$. This may be operative if the singlet–triplet energy gap between two ion radical pairs is small.

(49) Calculated values using kinetic parameters reported in ref 50.

(50) Dowd, P.; Chow, M. *J. Am. Chem. Soc.* **1977**, *99*, 6438–6440.

(51) Salem, L.; Rowland, C. *Angew. Chem., Int. Ed. Engl.* **1972**, *11*, 92–111.

(ii) **1,1-Bis(4-methoxyphenyl)-2-methylenespiro[2.2]pentane (2)**: mp 62 °C (colorless needles from EtOH); ^1H NMR (90 MHz, CCl_4) δ 1.13 (m, 2 H), 1.23 (m, 2 H), 3.70 (s, 6 H), 5.16 (s, 1 H), 5.48 (s, 1 H), 6.65 (m, 4 H), 7.00 (m, 4 H); MS (80 °C, 25 eV) m/z (relative intensity) 293 (10), 292 (40, M^+), 277 (23), 265 (23), 264 (100), 249 (28), 233 (19), 229 (12), 221 (13), 178 (16), 121 (15); UV (CH_3CN , $\lambda_{\text{max}}/\text{nm}$, $\epsilon/\text{M}^{-1}\text{cm}^{-1}$) 235 (19800), 277 (2860).

(iii) **1-Cyclopropylidene-2,2-bis(4-methoxyphenyl)cyclopropane (3)**: mp 41 °C (colorless solid from *n*-hexane); ^1H NMR (90 MHz, CCl_4) δ 1.27 (m, 4 H), 1.81 (m, 2 H), 3.70 (s, 6 H), 6.67 (m, 4 H), 7.07 (m, 4 H); MS (80 °C, 25 eV) m/z (relative intensity) 292 (6, M^+), 264 (30), 220 (18), 205 (100), 176 (52). This material was labile at room temperature and thus stored in a freezer under nitrogen.

(iv) **2-(4-Methoxyphenyl)-1-methylenecyclopropane (4)**: bp 45–47 °C (1 Torr); ^1H NMR (400 MHz, CDCl_3) δ 1.13 (m, 1 H), 1.68 (m, 1 H), 2.57 (m, 1 H), 3.78 (s, 3 H), 5.56–5.57 (m, 2 H), 6.81 (AA'BB', $J = 8$ Hz, 2 H), 7.08 (AA'BB', $J = 8$ Hz, 2 H); ^{13}C NMR (100 MHz, CDCl_3) δ 14.14, 19.40, 55.25, 104.35, 113.78 (2 C), 127.42 (2 C), 133.78, 135.58, 157.89; MS (70 eV) m/z (relative intensity) 160 (94, M^+), 159 (100).

(v) **(Z)-1-Ethylidene-2-(4-methoxyphenyl)cyclopropane (Z-5)**: colorless oil; ^1H NMR (200 MHz, CDCl_3) δ 1.06 (m, 1 H), 1.65 (m, 1 H), 1.79 (m, 3 H), 2.54 (m, 1 H), 3.78 (s, 3 H), 5.94 (m, 1 H), 6.81 (AA'BB', $J = 8.8$ Hz, 2 H), 7.04 (AA'BB', $J = 8.8$ Hz, 2 H); ^{13}C NMR (50 MHz, CDCl_3) δ 14.69, 16.98, 18.65, 55.24, 113.84 (2 C), 114.69, 126.42, 127.33 (2 C), 134.31, 157.81; UV (CH_2Cl_2 , λ_{max}) 296 nm.

(vi) **(E)-1-Ethylidene-2-(4-methoxyphenyl)cyclopropane (E-5)**: colorless oil; ^1H NMR (200 MHz, CDCl_3) δ 1.03 (m, 1 H), 1.61 (m, 1 H), 1.88 (m, 3 H), 2.53 (m, 1 H), 3.77 (s, 3 H), 5.96 (m, 1 H), 6.80 (AA'BB', $J = 8.6$ Hz, 2 H), 7.06 (AA'BB', $J = 8.6$ Hz, 2 H); ^{13}C NMR (50 MHz, CDCl_3) δ 13.03, 16.78, 19.31, 55.27, 113.78 (2 C), 114.44, 126.88, 127.48 (2 C), 134.66, 157.88; MS (70 eV) m/z (relative intensity) 174 (54, M^+), 159 (100), 143 (25), 128 (24); UV (CH_2Cl_2 , $\lambda_{\text{max}}/\text{nm}$) 298.

Analyses of Time-Dependent Change in the Product Ratios for the PET Degenerate Methylenecyclopropane Rearrangement of d_2 -1. A 0.5 mL CD_3CN solution containing d_2 -1 (0.05 mmol, 0.1 M) and sensitizer (0.01 mmol, 0.02 M^{52} for DCA, 0.0005 mmol, 0.001 M for TCNB, 0.005 mmol, 0.01 M for $\text{NMQ}^+\text{BF}_4^-$) with or without cosensitizer (0.1 mmol, 0.02 M for BP- d_{10} and TOL- d_8) in a Pyrex NMR tube was degassed by five repeated freeze (−196 °C)–pump (10^{-2} Torr)–thaw (0 °C) cycles and then sealed at 10^{-2} Torr. Similar sample solution in CD_2Cl_2 or C_6D_6 was just saturated with nitrogen by moderate bubbling for 5 min. These solutions were irradiated through a cutoff filter ($\lambda > 360$ nm for DCA or $\lambda > 300$ nm for TCNB and $\text{NMQ}^+\text{BF}_4^-$) with a 2 kW Xe lamp at 20 ± 1 °C. The ratios, d_2 -1: d_2 -1', during the photoreaction were determined by 200 MHz ^1H NMR analyses. Results are shown in Table 2.

Analyses of Time-Dependent Change in the Product Ratios for the PET Methylenecyclopropane Rearrangement of 2. A 0.5 mL CD_3CN solution containing 2 (0.05 mmol, 0.1 M) and sensitizer (0.01 mmol, 0.02 M^{52} for DCA, 0.0005 mmol, 0.001 M for TCNB, 0.005 mmol, 0.01 M for $\text{NMQ}^+\text{BF}_4^-$) with or without cosensitizer (0.1 mmol, 0.02 M for BP- d_{10} and TOL- d_8) in a Pyrex NMR tube was saturated with nitrogen by moderate bubbling for 5 min. These solutions were irradiated through a cutoff filter ($\lambda > 360$ nm for DCA or $\lambda > 300$ nm for TCNB and $\text{NMQ}^+\text{BF}_4^-$) with a 2 kW Xe lamp at 20 ± 1 °C. The ratios, 2:3, during the photoreaction were determined by 200 MHz ^1H NMR analyses.

General Procedure of the PET Reactions of 1, 2, and 3 under Oxygen. A 5 mL solution containing substrate (0.05 mmol, 0.01 M)

and sensitizer (0.01 mmol, 0.002 M^{52} for DCA, 0.0005 mmol, 0.0001 M for TCNB, 0.005 mmol, 0.001 M for $\text{NMQ}^+\text{BF}_4^-$) with or without cosensitizer (0.1 mmol, 0.02 M for BP and TOL) in a Pyrex test tube (diameter 1 cm) was saturated with oxygen by bubbling for 5 min. These solutions were irradiated through a cutoff filter ($\lambda > 360$ nm for DCA or $\lambda > 300$ nm for TCNB and $\text{NMQ}^+\text{BF}_4^-$) with a 2 kW Xe lamp at 20 ± 1 °C under oxygen. The yields of products were determined by ^1H NMR analyses after removal of the solvent and cosensitizer by evaporation in vacuo and column chromatography, respectively. The products 8² and 9 were separated from the reaction mixture by further chromatography. Physical data of 9 are as follows.

Compound 9: colorless oil; ^1H NMR (90 MHz, CCl_4) δ 0.93 (m, 2 H), 1.02 (m, 2 H), 3.75 (s, 6 H), 4.78 (m, 2 H), 6.70 (m, 4 H), 7.13 (m, 4 H); ^{13}C NMR (50 MHz, CDCl_3) δ 1.82 (t), 2.98 (t), 55.23 (q), 74.61 (t), 91.51 (s), 113.25 (d), 114.46 (s), 129.43 (d), 132.96 (s), 137.94 (s), 159.61 (s); MS (90 °C, 25 eV) m/z (relative intensity) 325 (10), 324 (33, M^+), 308 (21), 292 (8), 243 (74), 205 (52), 135 (100).

TCNB-Sensitized Photoreaction of 1 with in the Presence of DCDMF. A dichloromethane solution (3 mL) containing 1 (13.3 mg, 0.05 mmol), TCNB (2.7 mg, 0.015 mmol), and DCDMF (19.4 mg, 0.1 mmol) in a Pyrex test tube (diameter 1 cm) was saturated with argon by bubbling for 5 min. The sample solution was irradiated for 2 h at 20 ± 1 °C under argon with a 2 kW Xe lamp through a cutoff filter ($\lambda > 330$ nm). The yields of products were determined by ^1H NMR analyses after evaporation in vacuo. Details of the procedure to separate *trans*-12, *cis*-12, and 13 are described below.

Separation of *trans*- and *cis*-1,2-Dicarbomethoxy-1,2-dicyano-3,3-bis(4-methoxyphenyl)-4-methylenecyclopentane (*trans*-12 and *cis*-12) and *trans*-1,2-Dicarbomethoxy-1,2-dicyano-4-(bis(4-methoxyphenyl)methylene)cyclopentane (13). An acetonitrile solution (20 mL) containing 1 (226 mg, 0.85 mmol), DCA (9.7 mg, 0.042 mmol), and DCDMF (180 mg, 0.93 mmol) in a Pyrex test tube (diameter 5 cm) was saturated with argon by bubbling for 5 min. The sample solution was irradiated for 15 h at 20 ± 1 °C under argon with a 2 kW Xe lamp through a cutoff filter ($\lambda > 360$ nm). Removal of the solvent in vacuo gave 420 mg of a brown oil. Repetitive HPLC followed by recrystallization gave pure *trans*-12 (35 mg, 0.076 mmol, 9% yield), *cis*-12 (43 mg, 0.093 mmol, 11% yield), and 13 (12 mg, 0.026 mmol, 3% yield).

***trans*-12:** mp 143–146 °C (colorless cubes from CHCl_3 –*n*-hexane); ^1H NMR (400 MHz, CDCl_3) δ 3.37 (d, $J = 16.0$ Hz, 1 H), 3.50 (dd, $J = 16.0$, 2.1 Hz, 1 H), 3.62 (s, 3 H), 3.78 (s, 3 H), 3.83 (s, 3 H), 3.85 (s, 3 H), 4.85 (d, $J = 1.2$ Hz, 1 H), 5.66 (dd, $J = 2.1$, 1.2 Hz, 1 H), 6.79 (AA'BB', $J = 6.8$, 2.0 Hz, 2 H), 6.91 (AA'BB', $J = 6.8$, 2.0 Hz, 2 H), 7.19 (AA'BB', $J = 6.8$, 2.4 Hz, 2 H), 7.57 (AA'BB', $J = 6.8$, 2.4 Hz, 2 H); ^{13}C NMR (100 MHz, CDCl_3) δ 42.25, 53.37, 54.06, 54.79, 55.21, 55.23, 66.19, 69.34, 113.11 (2 C), 113.23 (2 C), 115.70, 116.52, 117.80, 131.17 (2 C), 131.46 (2 C), 131.67, 131.76, 148.36, 159.13, 163.88, 164.63; MS (70 eV) m/z (relative intensity) 460 (M^+ , 100); IR (KBr) 2232, 1760 cm^{-1} .

***cis*-12:** mp 161–162 °C (colorless cubes from CHCl_3 –*n*-hexane); ^1H NMR (400 MHz, CDCl_3) δ 3.36 (ddd, $J = 16.8$, 2.0, 2.0 Hz, 1 H), 3.42 (s, 3 H), 3.80 (s, 3 H), 3.82 (s, 3 H), 3.83 (s, 3 H), 3.91 (ddd, $J = 16.8$, 2.0, 2.0 Hz, 1 H), 4.89 (dd, $J = 2.0$, 2.0 Hz, 1 H), 5.54 (dd, $J = 2.0$, 2.0 Hz, 1 H), 6.82 (AA'BB', $J = 9.2$, 2.0 Hz, 2 H), 6.89 (AA'BB', $J = 9.2$, 2.2 Hz, 2 H), 7.20 (AA'BB', $J = 9.2$, 2.4 Hz, 2 H), 7.67 (AA'BB', $J = 9.2$, 2.4 Hz, 2 H); ^{13}C NMR (100 MHz, CDCl_3) δ 41.64, 53.81, 53.93, 54.50, 55.23, 55.26, 65.90, 69.87, 113.10 (2 C), 113.26 (2 C), 116.03, 116.19, 116.68, 130.75, 131.09 (2 C), 131.53, 131.83 (2 C), 148.86, 159.13, 159.31, 165.56, 166.63; MS (70 eV) m/z (relative intensity) 460 (M^+ , 100); IR (KBr) 2236, 1748, 1733 cm^{-1} .

Compound 13: mp 49–50 °C (colorless cubes from ether); ^1H NMR (400 MHz, CDCl_3) δ 3.32 (d, $J = 18.2$ Hz, 2 H), 3.42 (d, $J = 18.2$ Hz, 2 H), 3.81 (s, 6 H), 3.92 (s, 6 H), 6.86 (AA'BB', $J = 8.8$, 2.0 Hz, 4 H), 7.08 (AA'BB', $J = 8.8$, 2.0 Hz, 4 H); ^{13}C NMR (100 MHz, CDCl_3) δ 41.54 (2 C), 53.81 (2 C), 54.56 (2 C), 55.26 (2 C), 113.85 (4 C), 115.41

(52) The sample solution was slightly suspended with DCA. The actual concentrations of DCA are the saturated ones, which are ca. 4×10^{-3} , 2×10^{-3} , and 3×10^{-3} M at 20 °C, in acetonitrile, dichloromethane, and benzene, respectively.⁵³

(2 C), 126.66 (2 C), 129.97 (4 C), 133.40 (2 C), 139.98 (2 C), 156.91 (2 C), 164.77 (2 C); MS (70 eV) m/z (relative intensity) 460 (M^+ , 100); IR (KBr) 2216, 1752 cm^{-1} .

Nanosecond TR Absorption Spectroscopy of PET Reactions on Laser Flash Photolysis. A sample solution (2–4 mL) containing a substrate (1 mM), a sensitizer, whose absorbance was adjusted to be ca. 1.5 at the excitation wavelength, and a cosensitizer (0.2 M) in a glass cell was saturated with argon, nitrogen, or oxygen by bubbling for 5 min just before use. The sample solution was irradiated with 10 ns pulse beams obtained from an Excimer or YAG laser system. The probe assembly consisted of a monitoring lamp, a polychromator equipped with an image intensifier coupled with an image sensor, and a personal computer. The monitoring beam was adjusted to be perpendicular to the excitation pulse. The combination of a monochromator, a photomultiplier tube, and a digitizing oscilloscope was used for the measurements of decay kinetics. An analogous laser flash photolysis system has been described elsewhere.⁵⁴

Observation of 10^\bullet on Laser Flash Photolysis. Radical 10^\bullet was generated by laser flash photolysis (excimer, XeCl, $\lambda_{\text{ex}} = 308 \text{ nm}$) of 1,1-bis(4-methoxyphenyl)ethane (0.022 M) with di-*tert*-butyl peroxide (0.5 M) in acetonitrile and dichloromethane. The system for nanosecond TR absorption spectroscopy is similar to that for PET reactions.

(53) Ikeda, H.; Aburakawa, N.; Tanaka, F.; Fukushima, T.; Miyashi, T. *Eur. J. Org. Chem.* **2001**, 3445–3452.

(54) Ushida, K.; Nakayama, T.; Nakazawa, T.; Hamanoue, K.; Nagamura, T.; Mugishima, A.; Sakimukai, S. *Rev. Sci. Instrum.* **1989**, 60, 617–623.

Energy Determination by TR Photoacoustic Calorimetry. Details of the experimental procedure for photoacoustic calorimetry have been given previously.^{1a,33a,b,35b} Values were obtained by at least two separate runs, and errors are within 1σ . A chart of the photoacoustic calorimetry, waveforms, and deconvolution fitting parameters for the 1/DCA-BP system is available as Supporting Information in ref 6.

Acknowledgment. We gratefully acknowledge financial support by a Grant-in-Aid for Scientific Research on Priority Areas (417) and others (Nos. 08740560, 09740536, 10640507, 122440173, and 14050008) from the Ministry of Education, Culture, Sports, Science, and Technology (MEXT) of the Japanese Government. We also acknowledge Professors J. A. Berson (Yale University) and J. P. Dinnocenzo (University of Rochester) for valuable discussions, Professor M. Kamata (Niigata University) for informing us of a new procedure for the preparation of **1**, and Dr. Y. Hoshi (Tohoku University) for technical assistance with laser flash photolysis experiments.

Supporting Information Available: Details of the experiment including general methods, syntheses, and physical data for substrates, and verifying the energy of $^36^{\bullet\bullet}$ (PDF). This material is available free of charge via the Internet at <http://pubs.acs.org>.

JA0277982